

# Environmental and Experimental Botany

## Polyploidy-mediated divergent light-harvesting and photoprotection strategies under temperature stress in a Mediterranean carnation complex

--Manuscript Draft--

<b>Manuscript Number:</b>	EEB_2019_1190R1
<b>Article Type:</b>	Research Paper
<b>Keywords:</b>	Autopolyploidy; Dianthus broteri; Photochemical efficiency; Energy fluxes; Temperature stress; Environmental constraints
<b>Corresponding Author:</b>	Javier López-Jurado Departamento de Biología Vegetal y Ecología, Facultad de Biología, Universidad de Sevilla Seville, Spain
<b>First Author:</b>	Javier López-Jurado
<b>Order of Authors:</b>	Javier López-Jurado Francisco Balao Enrique Mateos-Naranjo
<b>Abstract:</b>	<p>Polyploidy can induce physiological novelties with adaptive potential, which may influence the range of environmental conditions that a neopolyploid tolerates. <i>Dianthus broteri</i> (Caryophyllaceae) is an autopolyploid complex that comprises four ploidy levels (2<math>\times</math>, 4<math>\times</math>, 6<math>\times</math> and 12<math>\times</math>) with separate distributions in the Iberian Peninsula, occupying different ecological niches along a gradient of temperature and aridity. We designed an experimental approach to disentangle the differential photochemical responses to temperature (from -3 °C to 53 °C) among <i>D. broteri</i> cytotypes by the measurement of leaf chlorophyll fluorescence. Our results showed higher energy fluxes, Fv/Fm and delayed fluorescence values along low and mild temperature levels in lower ploidies (2<math>\times</math> and 4<math>\times</math>) compared to higher ones (6<math>\times</math> and 12<math>\times</math>). This pattern would allow lower cytotypes to enhance their photosynthetic apparatus functionality in environmentally non-stressful habitats as those they inhabit. Contrarily, the 6<math>\times</math> cytotype exhibited the overall lowest energy fluxes based on a reduced absorption while maximizing its flux ratios. Moreover, the 12<math>\times</math> cytotype had notably high dissipation fluxes to ensure photoprotection, maintaining low but constant photochemical efficiency. These latter strategies would cause the reduction of photosynthetic capacities but help higher ploidies to tolerate the semi-arid Mediterranean environmental conditions with high temperatures under which they live.</p>
<b>Suggested Reviewers:</b>	Bernardo Duarte baduarte@fc.ul.pt  Giacomo Puglielli giacomo.puglielli@gmail.com  Pamela Soltis psoltis@flmnh.ufl.edu
<b>Response to Reviewers:</b>	

## Highlights

- *D. broteri* showed inter-cytype photochemical differences under heat and cold.
- An approach based on chlorophyll fluorescence in detached leaves was found suitable.
- 2× and 4× cytypes showed overall higher energy fluxes than 6× and 12× ones.
- Light-harvesting and photoprotective responses to temperature stress were found.
- Each cytype exhibited a divergent strategy related to its environmental niche.

1 **Polyploidy-mediated divergent light-harvesting and photoprotection strategies**  
2 **under temperature stress in a Mediterranean carnation complex**

3

4 Javier López-Jurado\*, Francisco Balao, Enrique Mateos-Naranjo

5

6 Departamento de Biología Vegetal y Ecología, Facultad de Biología, Universidad de  
7 Sevilla, Apdo. 1095, E-41080 Sevilla, Spain

8

9 \*Corresponding author.

10 **E-mail address:** javlopez@us.es

11 **Tel.:** +34 95 4552763

12 **ABSTRACT**

13 Polyploidy can induce physiological novelties with adaptive potential, which may  
14 influence the range of environmental conditions that a neopolyploid tolerates. *Dianthus*  
15 *broteri* (Caryophyllaceae) is an autopolyploid complex that comprises four ploidy levels  
16 (2×, 4×, 6× and 12×) with separate distributions in the Iberian Peninsula, occupying  
17 different ecological niches along a gradient of temperature and aridity. We designed an  
18 experimental approach to disentangle the differential photochemical responses to  
19 temperature (from -3 °C to 53 °C) among *D. broteri* cytotypes by the measurement of  
20 leaf chlorophyll fluorescence. Our results showed higher energy fluxes,  $F_v/F_m$  and  
21 delayed fluorescence values along low and mild temperature levels in lower ploidies  
22 (2× and 4×) compared to higher ones (6× and 12×). This pattern would allow lower  
23 cytotypes to enhance their photosynthetic apparatus functionality in environmentally  
24 non-stressful habitats as those they inhabit. Contrarily, the 6× cytotype exhibited the  
25 overall lowest energy fluxes based on a reduced absorption while maximizing its flux  
26 ratios. Moreover, the 12× cytotype had notably high dissipation fluxes to ensure  
27 photoprotection, maintaining low but constant photochemical efficiency. These latter  
28 strategies would cause the reduction of photosynthetic capacities but help higher  
29 ploidies to tolerate the semi-arid Mediterranean environmental conditions with high  
30 temperatures under which they live.

31

32 *Keywords:*

33 Autopolyploidy; *Dianthus broteri*; Photochemical efficiency; Energy fluxes;  
34 Temperature stress; Environmental constraints

## 35 1. Introduction

36 Polyploidy is the state of organisms with more than a pair of chromosome sets.  
37 In plants, it is extensively documented that polyploidy-associated novelties and  
38 subsequent local adaptation can alter phenotype and fitness through morphological,  
39 reproductive and/or physiological shifts (Levin, 2002; Ramsey and Ramsey, 2014). In  
40 fact, abiotic tolerances have been addressed as one of the key factors promoting habitat  
41 differentiation in polyploids relative to their diploid progenitors (Marchant et al., 2016).  
42 However, there is an evident lack of information in a context of physiology, functional  
43 traits or ecology regarding polyploid systems (Soltis et al., 2016). The few physiological  
44 studies on polyploids show an important bias towards the use of diploid-tetraploid  
45 comparisons (e.g. Li et al., 2011; Vyas et al., 2007) and, therefore, new approaches with  
46 high polyploid complexes are required to test the significance of increases in ploidy in  
47 such conclusions. Moreover, a common confounding factor in these studies is the  
48 allopolyploidy (polyploids originated from interspecific hybridization; e.g. Coate et al.,  
49 2012; Martínez et al., 2018) which produce transgressive phenotypes and diverse  
50 combinations of traits of the hybridizing partners (Seehausen, 2004). For this reason,  
51 new studies are also needed to ascertain if the adaptive advantage of allopolyploids over  
52 diploids across a broad range of environments could be extended to wild autopolyploids  
53 (polyploids originated from a single species), as recommended by Wei et al. (2019).

54 *Dianthus broteri* (Caryophyllaceae) is a recently radiated autopolyploid complex  
55 of perennial herbaceous plants with four different cytotypes (2 $\times$ , 4 $\times$ , 6 $\times$  and 12 $\times$ ; Balao  
56 et al., 2010, 2009). Endemic to the Iberian Peninsula, this complex encompasses a  
57 considerable diversity of microhabitats, but each cytotype is distributed in a different  
58 geographic range and always in single-ploidy populations (Balao et al., 2009). Across  
59 *D. broteri* cytotypes, several polyploidy-associated shifts have been identified in  
60 morphological traits (vegetative and reproductive organs; Balao et al., 2011) and global  
61 cytosine methylation levels (Alonso et al., 2016). Furthermore, it has been addressed  
62 that *D. broteri* distribution is greatly constrained by abiotic factors, essentially  
63 temperature, water availability and soil properties. Thus, environmental gradients  
64 fostered niche evolution in this polyploid complex causing lower cytotypes (2 $\times$  and 4 $\times$ )  
65 to occupy broader niches with milder environmental conditions compared to the higher  
66 ploidies (6 $\times$  and 12 $\times$ ), which are distributed in warmer, drier and more restricted niches

67 (López-Jurado et al., 2019a). Specifically, the dodecaploid cytotype (*Dianthus*  
68 *inoxianus*; Gallego, 1986) has received special attention because it is the highest-order  
69 polyploidy category in the genus. Moreover, it is considered threatened (Balao et al.,  
70 2007) and probably supports key vulnerable ecosystem functions (López-Jurado et al.,  
71 2019b). This cytotype also showed a remarkable high tolerance to physical damage to  
72 roots (López-Jurado et al., 2019b) and water stress (López-Jurado et al., 2016). In fact,  
73 an ecophysiological characterization of *D. inoxianus* under drought events revealed a  
74 great integrity of its photochemical apparatus, as indicated by the maintenance of  
75 photochemical efficiency, non-biochemical limitations and pigments concentrations  
76 stability (López-Jurado et al., 2016).

77         Given the distribution range of *D. broteri* cytotypes in the western  
78 Mediterranean basin, climate change effects will exert a great constraint on them. In the  
79 Iberian Peninsula and the entire Mediterranean area, significant changes in temperature  
80 have been addressed (Fonseca et al., 2016; Giorgi and Lionello, 2008), as extreme  
81 temperature events (Abaurrea et al., 2018; Lau and Nath, 2014). Short heat and cold  
82 episodes trigger some well described mechanisms in plant metabolism and might have  
83 important consequences on plant phenology, reproduction and physiology (Hatfield and  
84 Prueger, 2015; Menzel et al., 2011; Pérez-Romero et al., 2019). These response  
85 processes are shared by both temperature stresses (Kaplan et al., 2004) and involve,  
86 among others, the synthesis of reactive oxygen species (ROS), antioxidants, abscisic  
87 acid (ABA), shock proteins and changes in fatty acids composition (Maeda et al., 2006;  
88 Penfield, 2008; Wahid et al., 2007). Eventually, the photosynthetic rate decreases due to  
89 the reduced RuBisCO activation and the dysfunction of photosystems (Ensminger et al.,  
90 2006; Hikosaka et al., 2006; Mathur et al., 2014).

91         One of the most powerful and widely used methods to monitor this type of fine-  
92 scale plant photosynthetic reactions is the chlorophyll fluorescence analysis (Ducruet et  
93 al., 2007). This technique provides a precise assessment of the photosynthetic apparatus  
94 performance in response to environmental stresses by means of simple, sensitive and  
95 non-invasive measurements (Baker, 2008; Kalaji et al., 2016). On the one hand, the  
96 “fluorescence transient” (i.e. Kautsky curve) estimated from prompt chlorophyll *a*  
97 emission kinetics is analyzed by the OJIP test, which informs about the stepwise energy  
98 fluxes (electron transport) through photosystems (Strasser et al., 2004). This test

99 represents an appropriate method to detect temperature stress (Xu et al., 2014) and,  
100 especially, the related maximum photochemical efficiency of PSII ( $F_v/F_m$ ) has been  
101 addressed as a selection criterion for tolerant species (Sharma et al., 2014, 2012). On the  
102 other hand, when prompt fluorescence has decayed, delayed fluorescence is emitted in  
103 the red infrared region of the spectrum (Goltsev et al., 2009). This emission is  
104 associated with many photosynthetic reactions and explains light-induced electron  
105 transfer and related events not measurable by other methods (Buchta et al., 2007). For  
106 this reason, delayed fluorescence has been widely used to detect plant responses to  
107 environmental stresses, including the temperature one (Goltsev et al., 2009; Guo and  
108 Tan, 2013), and as a tool for assessing the degree of chilling sensitivity in plants  
109 (Ducruet et al., 2007). Therefore, the joint measurement of both types of fluorescence  
110 has been recommended to obtain further insights into the effects of abiotic stress in  
111 plants (Oukarroum et al., 2013; Salvatori et al., 2014). In addition, the use of detached  
112 leaves would also be helpful for screening numerous samples as well as, eventually, will  
113 allow us to characterize the physiochemical shifts caused by temperature excluding  
114 other abiotic factors such as light, water and nutrient supply (Sharma et al., 2014).

115 Thus, the main aim of this study was to uncover the differential temperature  
116 stress-triggered photochemical mechanisms across high polyploid series, using the *D.*  
117 *broteri* autopolyploid complex as a model. Specifically, we hypothesized that there  
118 would be a link between photochemical strategies and the thermal niche of each  
119 cytotype. Therefore, higher cytotypes would have developed strong adaptations to cope  
120 with extreme heat events whereas lower ploidies would show less marked  
121 photochemical responses and better performances under cold and mild temperatures.

## 122 **2. Materials and methods**

### 123 *2.1. Plant material and experimental set-up*

124 The experiment was conducted using mature *Dianthus broteri* plants ( $n = 5$ , per  
125 ploidy level) from seeds collected during late summer 2017 in two natural populations  
126 of each cytotype. These plants were grown for one year in 2.5 L pots filled with an  
127 organic commercial substrate (Gramoflor GmbH und Co. KG.) and perlite mixture (3:1)  
128 inside University of Seville Glasshouse General Services, with controlled temperature  
129 of 21-25 °C, 40-60% relative humidity, adequate irrigation with tap water and natural

130 illumination, being the maximum photosynthetic photon flux density (PPFD) level  
131 incident on leaves of  $1200 \mu\text{mol m}^{-2} \text{s}^{-1}$ .

132 In June 2019, following the methodology employed by Brestic et al. (2012) and  
133 Perera-Castro et al. (2018), fully developed leaves from each *D. broteri* cytotype were  
134 randomly selected, detached and placed inside individual small sealable plastic bags  
135 with a hydrated atmosphere to avoid evaporative loss. They were subsequently exposed  
136 to target temperature levels by submersing them in a refrigerated circulating water bath  
137 (Frigiterm-TFT-10, JP Selecta, Spain) with an accurate temperature control ( $\pm 0.1 \text{ }^\circ\text{C}$ )  
138 during 30 min. Subsequently, bags were removed from the bath and leaves were taken  
139 out of them and dried for 10 min at room temperature (c.  $24 \text{ }^\circ\text{C}$ ). During this time, we  
140 placed leaf clips in the middle part of the leaf blades to perform chlorophyll  
141 fluorescence measurements. All this procedure was performed in darkness. Sample  
142 leaves of all cytotypes were replaced for each temperature treatment and specific  
143 fluorescence methodology.

144 A total of nine different temperature levels were selected from extreme cold ( $-3$   
145  $^\circ\text{C}$ ) to extreme heat ( $53 \text{ }^\circ\text{C}$ ) in steps of  $7 \text{ }^\circ\text{C}$ . Lowest and highest temperature levels were  
146 based on extreme events recorded in the Iberian Peninsula, where natural *Dianthus*  
147 *broteri* populations occur (De Castro et al., 2005). To reach the negative temperature in  
148 a liquid state, we added 30% glycerol to water, which disrupts the formation of ice  
149 (Chang and Baust, 1991).

## 150 2.2. Prompt fluorescence measurements

151 The chlorophyll *a* fast kinetics (by the OJIP test) was measured in dark-adapted  
152 leaves for each temperature and cytotype combination ( $n = 10$ , two leaves per plant),  
153 using the pre-programmed OJIP protocols of FluorPen FP100 (Photo System  
154 Instruments, Czech Republic). Derived parameters for this fluorescence transient data  
155 were calculated according to Strasser et al. (2004).

156 Moreover, other dark-adapted sample leaves from each temperature and  
157 cytotype combination ( $n = 10$ , two leaves per plant) were used for the quantification of  
158 photosystem II efficiency parameters, using a portable modulated fluorimeter (FMS-2,  
159 Hansatech Instrument Ltd., UK) due to its higher saturating pulse intensity. Basal  
160 fluorescence in darkness ( $F_0$ ) was measured using a modulated beam ( $<0.05 \mu\text{mol m}^{-2} \text{s}^{-1}$



161 <sup>1</sup> for 1.8  $\mu\text{s}$ ) too small to cause significant physiological changes in the samples  
162 (Schreiber et al., 1986). The data stored were an average taken over a 1.6-second period.  
163 Maximum fluorescence ( $F_m$ ) was then estimated by applying a saturating actinic light  
164 pulse of  $10000 \mu\text{mol m}^{-2} \text{s}^{-1}$  for 0.8 s and it was recorded as the highest average of two  
165 consecutive points. Thus,  $F_0$  and  $F_m$  values were used to calculate variable fluorescence  
166 ( $F_v = F_m - F_0$ ) and maximum quantum efficiency of PSII photochemistry ( $F_v/F_m$ ).

### 167 2.3. Delayed fluorescence measurements

168 Additional leaves from all cytotypes were stuck in a black cardboard and  
169 maintained in darkness after their removal from the bath for each temperature treatment  
170 ( $n = 4$ ). Delayed fluorescence was detected using a plant imaging system (NightShade  
171 LB 985, Berthold Technologies, Germany) equipped with a deeply cooled CCD camera.  
172 Leaves were illuminated for 20 s with light supplied from far red (730 nm), red (660  
173 nm), green (565 nm) and blue (470 nm) LED panels at 2, 105, 40 and  $110 \mu\text{mol m}^{-2} \text{s}^{-1}$ ,  
174 respectively. Immediately after switching off the LEDs, delayed fluorescence was  
175 measured and the recorded intensities of light were converted in counts per second  
176 (cps). Data were then normalized to each leaf area to obtain comparable cps values  
177 across cytotypes and temperatures.

### 178 2.4. Statistical analyses

179 Among the numerous OJIP-derived parameters, we selected those related to  
180 energetic pathways due to the useful information under stress conditions that they  
181 provide (Duarte et al., 2015). Specifically, we assessed PSII efficiency using  $F_0$  as well  
182 as  $F_v/F_m$  and we used electron probability variables (flux ratios;  $\phi_{E_0}$ ,  $\phi_{D_0}$  and  $\psi_0$ ). In  
183 addition, we employed the energy transduction fluxes on a leaf cross-section basis  
184 (phenomenological fluxes; ABS/CS, TR/CS, ET/CS and DI/CS) because in a  
185 preliminary analysis we found significant differences in the density of reaction centers  
186 (RC/CS) within temperatures and cytotypes (two-way analysis of variance, ANOVA:  $P$   
187  $< 0.05$ ; see Table 1 for parameter description). Finally, we examined the proportion of  
188 active oxygen-evolving complexes (OECs) as they are the most sensitive components of  
189 the photosynthetic machinery to high temperatures (Allakhverdiev et al., 2008, and  
190 references cited therein).

191 Thus, the influence of ploidy level and temperature (both treated as factors; a  
 192 total of 36 combinations) on these variables as well as delayed fluorescence were  
 193 analyzed using two-way ANOVAs. Given that temperature largely affected all the  
 194 response variables ( $P < 0.05$ ), one-way ANOVAs using ploidy level as explanatory  
 195 variable were also performed within each temperature. Significant test results were  
 196 followed by *post hoc* Tukey's HSD tests ( $\alpha = 0.05$ ) to detect pairwise differences  
 197 among ploidy levels. All statistical analyses were performed in R software ver. 3.6.1 (R  
 198 Core Team 2019).

199 **Table 1**

200 Glossary of chlorophyll fluorescence parameters used in this study.

<b>Photosystem II efficiency</b>	<b>Description</b>
$F_0$	Basal fluorescence in dark-adapted leaves
$F_v/F_m$	Maximum quantum efficiency of PSII photochemistry
<b>Energy fluxes (Kautsky curves)</b>	
$\Phi_{Eo}$	Probability that an absorbed photon will move an electron into the electronic transport chain
$\Phi_{Do}$	Quantum yield of the non-photochemical reactions
$\Psi_0$	Probability of a PSII trapped electron to be transported from $Q_A$ to $Q_B$
ABS/CS	Absorbed energy flux per leaf cross-section
TR/CS	Trapped energy flux per leaf cross-section
ET/CS	Electron transport energy flux per leaf cross-section
DI/CS	Dissipated energy flux per leaf cross-section

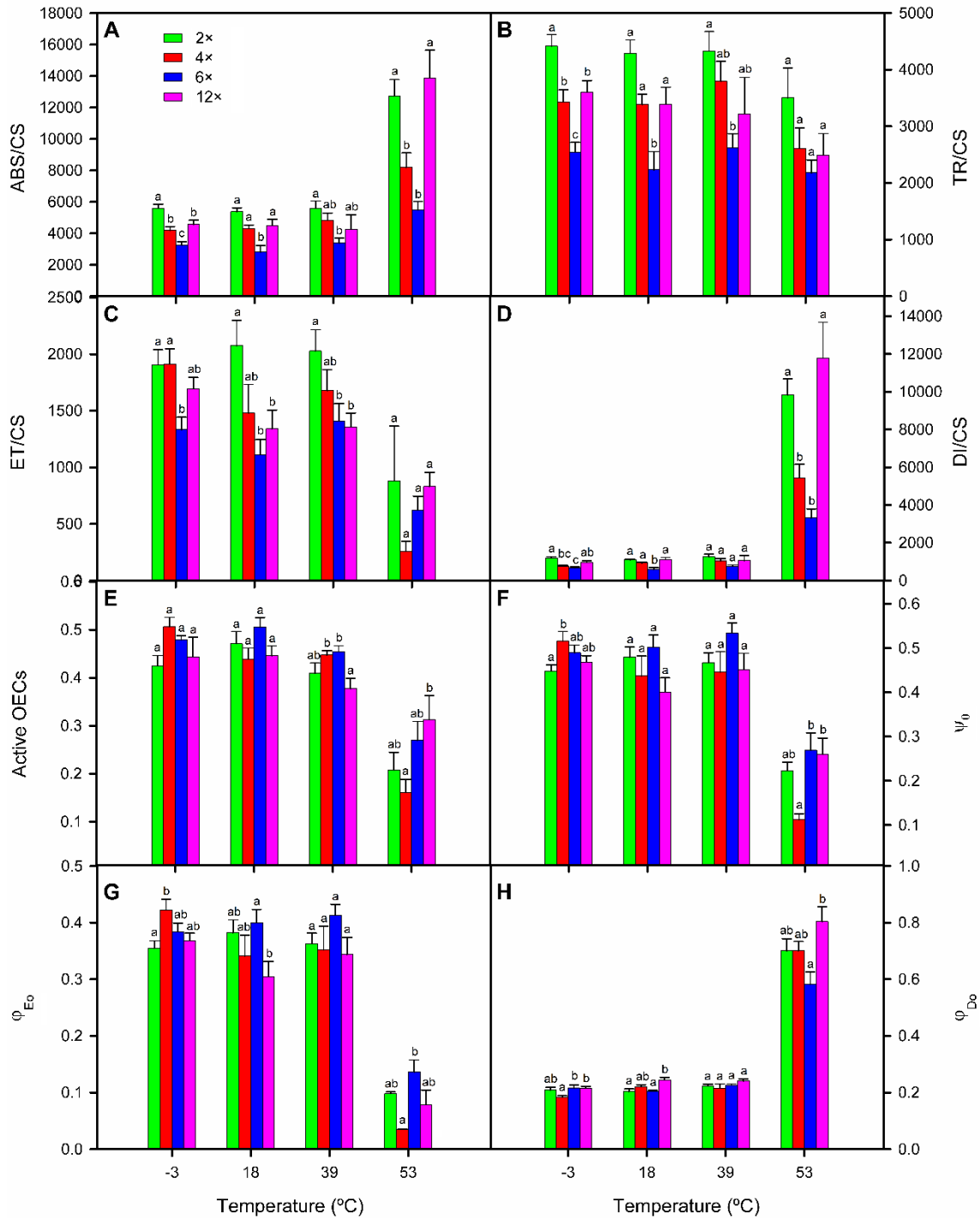
### 201 3. Results

202 All chlorophyll fluorescence parameters were broadly affected by temperature,  
203 especially by elevated temperature levels (two-way ANOVAs:  $P < 0.05$ ). Besides, there  
204 was a widespread inter-cytotype divergence in terms of photosystems functionality and  
205 energy fluxes, with remarkable differences in the Kautsky curves (Fig. S1). Along  
206 almost the whole temperature range, the greatest fluorescence values in all OJIP phases  
207 as well as energy fluxes (ABS/CS, TR/CS, ET/CS and DI/CS) were found in diploids  
208 and the lowest values were exhibited by hexaploids (Figs. 1A-D, S1). Oppositely to  
209 these constant trajectories, dodecaploids, and especially tetraploids, showed a  
210 considerably variable fluorescence emission under the changing temperature conditions  
211 (Figs. 1, S1, S2). Thus, the major effects mainly occurred under extremely high  
212 temperatures (i.e. 46 °C and 53 °C), when the shape of Kautsky curves changed and  
213 fluorescence decreased in the four cytotypes especially affecting the J-I-P (thermal)  
214 phase (Fig. S1). In fact, immediately prior to this phase, heat stress caused the  
215 appearance of the additional K band in Kautsky curves at around 1000  $\mu\text{s}$  (Fig. S1).  
216 This step was found for all the cytotypes but it was more pronounced in tetraploids due  
217 to their lower values of active oxygen-evolution complexes (OECs) at 53 °C compared  
218 to the rest of ploidies, especially the 12 $\times$  cytotype (one-way ANOVA,  $P < 0.05$ ; Fig.  
219 1E).

220 The mentioned differences among cytotypes were accompanied by a marked  
221 divergence in electron probability variables ( $\psi_0$ ,  $\phi_{E_0}$  and  $\phi_{D_0}$ ) at extreme temperatures (-  
222 3 °C and 53 °C) and at 18 °C (Fig. 1F-H). At the minimum temperature of exposure (-3  
223 °C), the 4 $\times$  cytotype showed enhanced flux ratios in terms of primary photochemistry,  
224 being the probability of an absorbed photon moving an electron into the electron  
225 transport chain ( $\phi_{E_0}$ ) as well as of its transport from  $Q_A$  to  $Q_B$  ( $\psi_0$ ), significantly higher  
226 than those of the other cytotypes (ANOVA: ploidy level,  $P < 0.05$ ; Fig. 1F, G).  
227 Furthermore, the 4 $\times$  cytotype had the lowest quantum yield of non-photochemical  
228 reactions ( $\phi_{D_0}$ ; Fig. 1H). In comparison with tetraploids, diploids showed greater  
229 absorbed (ABS/CS), trapped (TR/CS) and dissipated (DI/CS) energy fluxes (Fig. 1A, B,  
230 D), but not transported ones (ET/CS; Fig. 1C). At subsequent temperatures (4 °C to 25  
231 °C), the 4 $\times$  cytotype decreased its electron probability variables of primary  
232 photochemistry (Fig. S2F, G) but increased the four phenomenological energy fluxes,

233 making them similar to those of the 2× cytotype (Figs. 1A-D, S2A-D). Under 32 °C, we  
234 found the opposite pattern to the one exhibited under -3 °C. In this case, the 4× cytotype  
235 showed significantly higher energy fluxes compared to the 2× cytotype, especially  
236 ET/CS (ANOVA: ploidy level,  $P < 0.05$ ; Fig. S2A-D). Moreover, the exposure to high  
237 temperatures led again to increasing higher energy fluxes of diploids compared to  
238 tetraploids, with greater ABS/CS, DI/CS and primary photochemistry ratios under 53 °C  
239 (ANOVA: ploidy level,  $P < 0.05$ ; Figs. 1, S2).

240         Regarding the two higher ploidy levels, the 6× cytotype showed a generalized  
241 pattern of low energy fluxes based on its notably low ABS/CS values (Fig. 1A-D).  
242 Moreover, this cytotype exhibited a clear tendency to higher electron probability rates  
243 relative to photochemical reactions compared to the rest of cytotypes from 18 °C to  
244 extreme heat, being significantly higher at 18 °C and 53 °C (ANOVA: ploidy level,  $P <$   
245  $0.05$ ; Fig. 1F, G). Likewise, the 12× cytotype mirrored a trend towards non-  
246 photochemical processes, as highlighted by enhanced DI/CS (Fig. 1D). It tended to be  
247 more pronounced with increasing temperatures (significant higher values at 32 °C and  
248 53 °C; Fig. S2D; Fig. 1D), being this dissipated energy flux also accompanied by a  
249 greater quantum yield ( $\phi_{D_0}$ ) at 18 °C and 53 °C (ANOVA: ploidy level,  $P < 0.05$ ; Fig.  
250 1H). Dodecaploids also showed a comparatively high  $\psi_0$  under the highest temperature  
251 condition (Fig. 1F). Finally, the described pattern of high dissipation under extreme heat  
252 congruently occurred also with the greatest absorbed energy flux (ANOVA: ploidy  
253 level,  $P < 0.05$ ; Fig. 1A) and fluorescence values in the Kautsky curves (Fig. S1), both  
254 of them similar to those of the 2× cytotype.



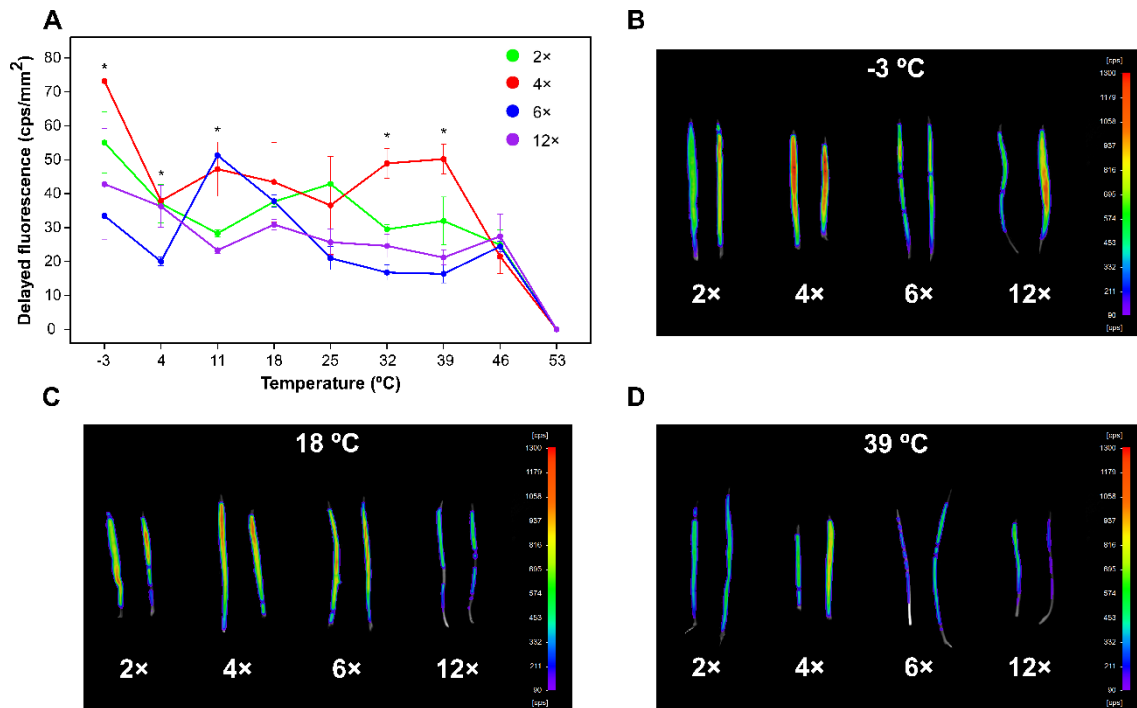
255

256 **Fig. 1.** Absorbed energy flux per leaf cross-section, ABS/CS (A), trapped energy flux  
 257 per leaf cross-section, TR/CS (B), transport energy flux per leaf cross-section, ET/CS  
 258 (C), dissipated energy flux per leaf cross-section, DI/CS (D), active oxygen-evolving  
 259 complexes, OECs (E), probability of a PSII trapped electron to be transported from Q<sub>A</sub>  
 260 to Q<sub>B</sub>, ψ<sub>0</sub> (F), probability that an absorbed photon will move an electron into the  
 261 electronic transport chain, φ<sub>E<sub>0</sub></sub> (G), and quantum yield of the non-photochemical

262 reactions,  $\phi_{D_0}$  (H), in dark-adapted leaves of the four *D. broteri* cytotypes exposed to  
263 four selected temperature levels of the complete range. Parameters were derived from  
264 measurements taken with FluorPen FP100. Values represent mean  $\pm$  standard error.  
265 Different letters indicate cytotypes that are significantly different from each other within  
266 each temperature level (one-way ANOVA:  $P < 0.05$ , Tukey's HSD test:  $\alpha = 0.05$ ).

267

268         Delayed fluorescence emissions were partly similar to prompt fluorescence ones.  
269 Along the temperature range, overall lower values were detected in 6 $\times$  and 12 $\times$   
270 cytotypes, especially in the first one, compared to 2 $\times$  and 4 $\times$  ploidies (Fig. 2A).  
271 Nevertheless, at mild temperature levels as 18 °C (Fig. 2C) and 25 °C, no significant  
272 differences between cytotypes were found (ANOVA: ploidy level,  $P > 0.05$ ; Table S1;  
273 Fig. 2A). Thus, delayed fluorescence became greater in the 4 $\times$  cytotype than in the  
274 remaining ploidies (ANOVA: ploidy level,  $P < 0.05$ ; Table S1) under extreme cold (-3  
275 °C; Fig. 2B) as well as under the high temperature levels 32 °C and 39 °C (Fig. 2A, D).  
276 Moreover, tetraploids showed higher values compared to at least one of the other  
277 cytotypes at cold temperatures (4 °C and 11 °C; Fig. 2A). However, unlike under  
278 extreme cold (Fig. 2B), the most elevated temperature (53 °C) dramatically reduced  
279 delayed fluorescence to zero values for all cytotypes (Fig. 2A). Remarkably, in the  
280 previous temperature level step from 39 °C to 46 °C, lower ploidies (2 $\times$  and 4 $\times$ ) suffered  
281 considerable delayed fluorescence decreases (of c. 22% and c. 57%, respectively)  
282 whereas higher ploidies (6 $\times$  and 12 $\times$ ) experienced increases (of c. 49% and c. 29%,  
283 respectively; Fig. 2A).



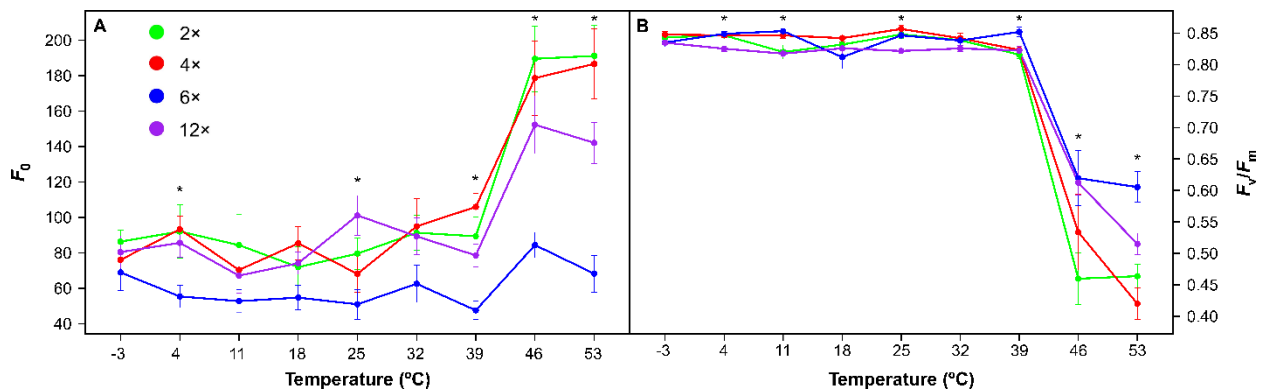
284

285 **Fig. 2.** Delayed fluorescence results in dark-adapted leaves of the four *D. broteri*  
 286 cytotypes exposed to nine different temperatures. Panel A presents cps values for each  
 287 ploidy level normalized to leaf area along the temperature range. Values represent mean  
 288  $\pm$  standard error. Asterisks indicate significant differences among cytotypes at each  
 289 temperature using one-way ANOVAs ( $P < 0.05$ ). Panels B, C and D show photographs  
 290 taken at  $-3$  °C,  $18$  °C and  $39$  °C, respectively, by the plant imaging system NightShade  
 291 LB 985. The color scale mirrors the detected counts per second (cps) of delayed  
 292 fluorescence emission in leaves.

293

294 As expected, the main pattern observed in the transient fluorescence emission  
 295 was repeated in the basal fluorescence ( $F_0$ ; Fig. 3A). Hexaploids exhibited the lowest  
 296 values across the temperature range, which were significantly lower than the remaining  
 297 cytotypes at  $4$  °C,  $25$  °C and, mostly, the three highest temperature levels (ANOVA:  
 298 ploidy level,  $P < 0.05$ ; Table S1; Fig. 3A). Moreover, all the cytotypes showed sharp  $F_0$   
 299 increases from  $39$  °C to  $46$  °C (Fig. 3A). However, it is noteworthy that these values  
 300 continued decreasing until  $53$  °C in the lower cytotypes ( $2\times$  and  $4\times$ ) whereas they  
 301 experienced subtle increases in  $6\times$  and  $12\times$  cytotypes (c. 19% and c. 7%, respectively;  
 302 Fig. 3A). From  $39$  °C to  $53$  °C, in contrast to  $F_0$  but similarly to prompt and delayed  
 303 fluorescence emissions, an additional sharp decrease occurred in the maximum quantum

304 efficiency of PSII photochemistry ( $F_v/F_m$ ; Fig. 3B). The four cytotypes shared this trend  
 305 although the lower ploidies showed greater  $F_v/F_m$  reductions with drops of c. 43%, c.  
 306 49%, c. 29% and c. 37% for 2×, 4×, 6× and 12× leaves, respectively. For this reason, 6×  
 307 and 12× ploidies had significantly higher  $F_v/F_m$  values than 2× and 4× at 46 °C and 53  
 308 °C, especially the hexaploid cytotype (ANOVA: ploidy level,  $P < 0.05$ ; Table S1). At  
 309 lower temperatures, little  $F_v/F_m$  differences among ploidy levels were recorded (only at  
 310 4 °C, 11 °C, 25 °C and 39 °C; ANOVA:  $P < 0.05$ ). These inter-cytotype differences in  
 311  $F_v/F_m$  were mainly due to lower values of the 12× cytotype when compared to the 6×  
 312 (Fig. 3B; Table S1). Nevertheless, from -3 °C to 39 °C,  $F_v/F_m$  values of all the cytotypes  
 313 remained remarkably constant, with average values ranging between 0.81-0.84 (Fig.  
 314 3B).



315

316 **Fig. 3.** Basal fluorescence,  $F_0$  (A), and maximum quantum efficiency of PSII  
 317 photochemistry,  $F_v/F_m$  (B), in dark-adapted leaves of the four *D. broteri* cytotypes  
 318 exposed to nine different temperatures. Parameters were derived from measurements  
 319 taken with the portable modulated fluorimeter FMS-2. Values represent mean  $\pm$   
 320 standard error. Asterisks indicate significant differences among cytotypes at each  
 321 temperature using one-way ANOVAs ( $P < 0.05$ ).

322

#### 323 4. Discussion

324 Our results demonstrated the existence of significant photochemical differences  
 325 among cytotypes through the entire temperature range tested. Notwithstanding specific  
 326 differences at some temperature levels,  $F_v/F_m$  values from -3 °C to 39 °C reflected a



327 relatively unaffected carbon metabolism and conversion to chemical energy in  
328 photosynthesis (Sharma et al., 2012). However, between 39 °C and 46 °C there seems to  
329 be a threshold for photosystems functionality. The impairment in such a fundamental  
330 process will influence the decay of many other processes downstream from primary  
331 photochemistry (Poudyal et al., 2019), as delayed fluorescence (Badretdinov et al.,  
332 2004). This latter process is, in turn, caused by the failure of important inner-protein  
333 proton movements in the thylakoid membrane (Buchta et al., 2007) and would lead to  
334 the loss of photosynthesis efficiency (Wang et al., 2007). Despite this general trend, we  
335 detected differences in energy fluxes and efficiencies among cytotypes to be more  
336 prominent at extreme temperatures (particularly, -3°C and 53 °C). These temperature  
337 levels triggered specific physiological responses to cope with the mentioned stress  
338 consequences.

339         Diploids and tetraploids occur in colder habitats than those of hexaploids and  
340 dodecaploids (López-Jurado et al., 2019a), which would explain their limited capacity  
341 to face extreme heat, dramatically decreasing  $F_v/F_m$  and delayed fluorescence emission.  
342 Additionally, lower cytotypes sharply increased basal fluorescence ( $F_0$ ) from elevated to  
343 severe heat (39 °C to both highest temperature levels), which is a sign of the irreversible  
344 aggregation of light-harvesting complexes and their dissociation from PSII (Yamane et  
345 al., 1997), an early indicator for damage in PSII (Mathur et al., 2011; Pollastri et al.,  
346 2019). Nevertheless, these lower cytotypes were capable to maintain an optimal  
347 photochemical functionality at low temperatures and mild conditions. Diploids  
348 enhanced total energy fluxes (ABS/CS, TR/CS, ET/CS and DI/CS) to maximize  
349 photosynthesis as confirmed by their high fluorescence values across temperatures in  
350 Kautsky curves, which were not accompanied by high flux ratios. Therefore, they  
351 demonstrated an offsetting between the amount of energy involved in fluorescence  
352 reactions and its use efficiency at the temperature range from low to moderate. This  
353 mechanism under chilling stress is described as ‘photoacclimation’ and avoids the  
354 damage of photosystems by balancing the energy absorbed with the energy metabolized  
355 and dissipated (Ensminger et al., 2006). However, the elevated absorption rate at high  
356 temperatures unbalances these processes because collected energy exceeds the capacity  
357 for photochemical reactions and the protective energy dissipation becomes necessary, as  
358 indicated by the enhanced DI/CS at 53 °C. This dissipated flux would cause the 2×  
359 cytotype to protect the donor side of PSII as demonstrated by its comparatively low

360 inactivation of OECs, which is the rate-limiting process in the photodamage to PSII  
361 (Takahashi and Murata, 2008).

362 In contrast, the 4× cytotype tolerated cold stress by decreasing its energy fluxes  
363 and maximizing their ratios for primary photochemistry and hence their delayed  
364 fluorescence intensity (Zhang and Xing, 2008). A possible explanation to this  
365 mechanism exhibited by the tetraploids would be the downregulation, redistribution or  
366 dissociation of antenna systems in order to harvest a lower light flux and promote  
367 energy-quenching mechanisms under these conditions (Rochaix, 2014; Xu et al., 2015).  
368 This strategy has been described in plant species exposed to cold temperatures, mostly  
369 in conifers distributed in boreal environments (Ensminger et al., 2004; Ottander et al.,  
370 1995) but also in *Arabidopsis thaliana* (Nellaepalli et al., 2012). Moreover, delayed  
371 fluorescence of this cytotype was constantly higher than the other ploidies and varied  
372 without abrupt changes between 4°C and 32 °C. This pattern indicated that the shift in  
373 light collection could be partly linked with the membrane fluidity of 4× thylakoids,  
374 which would not suffer phase transitions influenced by temperature (Havaux and  
375 Lannoye, 1983). Thus, this cytotype could be considered a chilling-resistant ploidy.  
376 Nevertheless, tetraploids exhibited an increase in delayed fluorescence emission at 32  
377 °C and 39 °C, which matches with a phase transition likely promoted by a remarkable  
378 structural flexibility of thylakoid membranes (Garab, 2014). Notably, energy fluxes of  
379 the 4× cytotype also increased and exceeded those of the 2× at 32 °C. This complex and  
380 flexible photochemical behavior of the 4× cytotype might be a consequence of its two  
381 independent lineages with unrelated evolutionary processes (Balao et al., 2010) and  
382 their different ecological niches (López-Jurado et al., 2019a). Recurrent origins of the  
383 tetraploids would have caused more diverse genetic and physiological properties  
384 (Weiss-Schneeweiss et al., 2013) which, in addition, would be especially regulated by  
385 local adaptation processes (McIntyre and Strauss, 2017). However, in this cytotype,  
386 severe heat caused a decrease of  $F_v/F_m$ , delayed fluorescence, energy fluxes and ratios  
387 (with low dissipation) as well as active OECs. These results suggested an excessive  
388 formation of reactive oxygen species (ROS), causing PSII photodamage (Yamamoto et  
389 al., 2008), the inhibition of its repair (Murata et al., 2007) and the inactivation of OECs  
390 (by lipid peroxidation; Song et al., 2006).

391 Additionally, 6× and 12× cytotypes exhibited straightforward mechanisms  
392 focused on the response to the highest temperatures. In this case, both higher cytotypes

393 showed a subtle  $F_0$  decrease at 53 °C after the marked increase from 39 °C to 46 °C. This  
394 reduction under extreme heat would support the dark reduction of  $Q_A$  as the main cause  
395 of the basal fluorescence rise, as demonstrated at similar temperatures (c. 50 °C;  
396 Yamane et al., 2000). Unlike the alleged irreversible changes attributed to lower  
397 ploidies, the redox state of  $Q_A$  would be reversed by reoxidation in higher ploidies  
398 (Yamane et al., 2000). This transition would also influence the greater maximum  
399 quantum efficiency of PSII photochemistry ( $F_v/F_m$ ) of 6× and 12× cytotypes against  
400 heat stress compared to 2× and 4×. Furthermore, the two higher ploidies showed a high  
401 preservation of active OECs of PSII, which could be protected by bicarbonate (Klimov  
402 et al., 1997) or the association of small heat-shock proteins (HSPs) with thylakoids  
403 (Heckathorn et al., 2002). In order to successfully complete their strategies, both higher  
404 cytotypes would have to regulate their photosynthetic capacities to concentrate the  
405 higher productivity-related rates in narrow periods of opportunity (Demmig-Adams et  
406 al., 2017).

407 Hexaploids additionally had low energy fluxes per leaf cross-section (especially  
408 the absorbed one) at the entire range of temperatures, based on reduced prompt and  
409 delayed fluorescence values. This behavior suggested more efficient photochemical  
410 machinery in relative terms, depicted by enhanced flux ratios and a high overall  $F_v/F_m$   
411 with a lessened reduction under heat stress. Jointly, these trends suggested that the 6×  
412 cytotype would base their photochemical strategy on the optimization of antenna size to  
413 prevent photoinhibition and increase photosynthetic efficiency (Adams and Demmig-  
414 Adams, 2004; Ort et al., 2011). This ‘avoidance’ adjustment of hexaploids was similar  
415 to the one exhibited by tetraploids under extreme cold but, in this case, seems to be a  
416 constitutive adaptation which allow their establishment in the highly nutrient-poor and  
417 light-exposed habitats that they inhabit (López-Jurado et al., 2019a, unpublished data).  
418 Congruently, the mentioned minimization of light-harvesting complexes has been  
419 addressed in other plants subjected to similar stresses (Logan et al., 1999; Morales et al.,  
420 2000).

421 Contrastingly, the 12× cytotype maintained overall higher energy fluxes than 6×,  
422 mostly at mild temperature conditions (from 18 °C to 32 °C), so probably light-  
423 harvesting antenna complexes are preserved and chlorophyll degradation is not acting as  
424 an underlying defense mechanism. Its overall high non-photochemical fluxes and yields

425 (DI/CS and  $\phi_{D_0}$ ), especially under severe heat, suggested that this cytotype is adapted to  
426 tolerate a considerable degree of photoinhibition. In fact, these joint results could reflect  
427 the well-addressed photoprotection of the photosynthetic apparatus via thermal  
428 dissipation to avoid ROS production (Demmig-Adams and Adams, 2006; Silva et al.,  
429 2015). In this ‘photoprotective’ strategy, excess energy would be dissipated through  
430 xanthophylls (zeaxanthin and antheraxanthin) retention and the rearrangement or  
431 degradation of PSII cores (Demmig-Adams and Adams, 2006). Together with the non-  
432 photochemical quenching (dissipated energy), linear electron transport downregulation  
433 (depicted here as ET/CS) is essential for protecting both photosystems and other  
434 chloroplast structures against photoinhibition damage (see Brestic et al., 2016 for  
435 temperature stress and Meng et al., 2016 for other abiotic stress -drought-). While the  
436 ET/CS decrease at high temperatures was shared by all cytotypes, the elevated DI/CS  
437 showed by 2× and 12× could be crucial to survive while absorbing excessive energy.  
438 The ‘photoprotective’ strategy and the previously mentioned  $F_0$  pattern would cause the  
439 12× cytotype to not suffer abrupt decreases in  $F_v/F_m$  under extreme temperatures and  
440 other abiotic stresses, as supported by the similar results obtained in a drought stress  
441 experiment (López-Jurado et al., 2016). Likewise, dodecaploids occur mostly in the  
442 understory of pine forests, with a much lower incoming radiation than hexaploids  
443 (López-Jurado et al., 2019b) so their strategy allows greater light absorption as well as  
444 photoprotection against environmental stresses.

445 Photochemical inter-cytotype differentiation is definitely associated with the  
446 environmental conditions of the niche that each cytotype occupies, which suggests an  
447 enhanced local adaptation and functional plasticity by means of polyploidization events  
448 (Ramsey, 2011) and epigenetic changes (Alonso et al., 2016; Song and Chen, 2015).  
449 These differences in physiological processes might be promoted by gene duplication as  
450 a result of polyploidization (Panchy et al., 2016). Duplicate retention of photosynthetic-  
451 associated genes, as those regulating the Calvin cycle and light-harvesting complexes,  
452 would then drive their functional divergence (neofunctionalization or  
453 subfunctionalization; Coate et al., 2011). The photochemical differentiation among *D.*  
454 *broteri* cytotypes was congruent with a previous pairwise diploid-polyploid comparison  
455 in citrus seedlings (Oustric et al., 2019) but cannot be generalized since there are  
456 examples of not a clear divergence (Pavlíková et al., 2017) as well as more effective  
457 adaptations in diploids (Guo et al., 2016). Furthermore, a similar study on cereals with

458 four different ploidy levels found greater photosynthetic capacities and more efficient  
459 antioxidant defense systems in higher ploidies under favorable conditions (6× and 8×;  
460 Mao et al., 2018).

461 Remarkably, although we detected that higher ploidies have developed specific  
462 photochemical processes to survive in extremely warm conditions, a divergence pattern  
463 was also found in favorable conditions (18 °C). The reduced performance of higher  
464 cytotypes suggested that they would be less competitive in a common environment with  
465 mild temperatures. As proposed by He et al. (2013), species interactions could shift  
466 under stress to facilitation or reduction in competition. Therefore, 6× and 12× cytotypes  
467 would have adapted to the absence of inter-cytype competition at their locations near  
468 to edges of the environmental gradients facilitating their establishment (López-Jurado et  
469 al., 2019a). However, the increase in frequency and severity of cold and heat episodes  
470 due to climate change, as indicated the most extreme predictions for Spain in the  
471 coming years (Furió and Meneu, 2011), could cause that 6× and 12× cytotypes would  
472 reach better performances compared to their low-cytype counterparts. Consequently,  
473 the current distribution of all ploidy levels would be compromised under climate change  
474 projections.

475 To sum up, the high autopolyploid complex *Dianthus broteri* gave us the  
476 opportunity to unravel the effect of successive genome duplications on physiological  
477 divergence and plasticity. In this case, highly specific photochemical adaptations to  
478 extreme heat were found in higher ploidy levels, which are distributed in warm and  
479 semi-arid environments. Notwithstanding the pattern cannot be generalized, this  
480 approach would shed light on the segregation pattern of cytotypes within other  
481 polyploid complexes and it would also be useful to provide new insights into their  
482 environmental preferences, niche evolution and ecological interactions, as well as to  
483 predict the evolution of the different cytotypes under climate change scenarios.

#### 484 **Acknowledgements**

485 We are grateful to the University of Seville Greenhouse General Service  
486 (CITIUS) for their collaboration and providing the facilities. Thanks to the anonymous  
487 referees for their constructive comments on a previous version of the manuscript. We

488 also thank the Department of Cell Biology at the University of Seville for allow us to  
489 use the water bath during the experiment.

#### 490 **Funding**

491 This study was supported by the Research Project PGC2018-098358-B-I00 from  
492 the Spanish MICINN and a predoctoral grant to J. López-Jurado from the VPPI-US  
493 (Fifth Research Plan from the University of Seville).

#### 494 **References**

495 Abaurrea, J., Asín, J., Cebrián, A.C., 2018. Modelling the occurrence of heat waves in  
496 maximum and minimum temperatures over Spain and projections for the period  
497 2031-60. *Glob. Planet. Change* 161, 244–260. doi:10.1016/j.gloplacha.2017.11.015

498 Adams, W.W., Demmig-Adams, B., 2004. Chlorophyll fluorescence as a tool to  
499 monitor plant response to the environment, in: Papageorgiou, G.C., Govindjee  
500 (Eds.), *Chlorophyll Fluorescence: A Signature of Photosynthesis*. Springer,  
501 Dordrecht, pp. 583–604. doi:10.1007/978-1-4020-3218-9\_22

502 Allakhverdiev, S.I., Kreslavski, V.D., Klimov, V. V., Los, D.A., Carpentier, R.,  
503 Mohanty, P., 2008. Heat stress: an overview of molecular responses in  
504 photosynthesis. *Photosynth. Res.* 98, 541–550. doi:10.1007/s11120-008-9331-0

505 Alonso, C., Balao, F., Bazaga, P., Pérez, R., 2016. Epigenetic contribution to successful  
506 polyploidizations: variation in global cytosine methylation along an extensive  
507 ploidy series in *Dianthus broteri* (Caryophyllaceae). *New Phytol.* 212, 571–576.  
508 doi:10.1111/nph.14138

509 Badretdinov, D.Z., Baranova, E.A., Kukushkin, A.K., 2004. Study of temperature  
510 influence on electron transport in higher plants via delayed luminescence method:  
511 experiment, theory. *Bioelectrochemistry* 63, 67–71.  
512 doi:10.1016/j.bioelechem.2003.12.003

513 Baker, N.R., 2008. Chlorophyll fluorescence: a probe of photosynthesis in vivo. *Annu.*

- 514 Rev. Plant Biol. 59, 89–113. doi:10.1146/annurev.arplant.59.032607.092759
- 515 Balao, F., Casimiro-Soriguer, R., Herrera, J., Talavera, S., 2007. *Dianthus inoxianus*  
516 Gallego, in: Bañares, Á., Blanca, G., Güemes, J., Moreno, J.C., Ortiz, S. (Eds.),  
517 Atlas y Libro Rojo de La Flora Vasculare Amenazada de España. Adenda 2006.  
518 Ministerio de Medio Ambiente y Medio Rural y Marino, Madrid, pp. 42–43.
- 519 Balao, F., Casimiro-Soriguer, R., Talavera, M., Herrera, J., Talavera, S., 2009.  
520 Distribution and diversity of cytotypes in *Dianthus broteri* as evidenced by  
521 genome size variations. Ann. Bot. 104, 965–973. doi:10.1093/aob/mcp182
- 522 Balao, F., Herrera, J., Talavera, S., 2011. Phenotypic consequences of polyploidy and  
523 genome size at the microevolutionary scale: a multivariate morphological  
524 approach. New Phytol. 192, 256–265. doi:10.1111/j.1469-8137.2011.03787.x
- 525 Balao, F., Valente, L.M., Vargas, P., Herrera, J., Talavera, S., 2010. Radiative evolution  
526 of polyploid races of the Iberian carnation *Dianthus broteri* (Caryophyllaceae).  
527 New Phytol. 187, 542–551. doi:10.1111/j.1469-8137.2010.03280.x
- 528 Brestic, M., Zivcak, M., Kalaji, H.M., Carpentier, R., Allakhverdiev, S.I., 2012.  
529 Photosystem II thermostability in situ: environmentally induced acclimation and  
530 genotype-specific reactions in *Triticum aestivum* L. Plant Physiol. Biochem. 57,  
531 93–105. doi:10.1016/j.plaphy.2012.05.012
- 532 Brestic, M., Zivcak, M., Kunderlikova, K., Allakhverdiev, S.I., 2016. High temperature  
533 specifically affects the photoprotective responses of chlorophyll b-deficient wheat  
534 mutant lines. Photosynth. Res. 130, 251–266. doi:10.1007/s11120-016-0249-7
- 535 Buchta, J., Grabolle, M., Dau, H., 2007. Photosynthetic dioxygen formation studied by  
536 time-resolved delayed fluorescence measurements - Method, rationale, and results  
537 on the activation energy of dioxygen formation. Biochim. Biophys. Acta -  
538 Bioenerg. 1767, 565–574. doi:10.1016/j.bbabi.2007.04.003
- 539 Chang, Z., Baust, J.G., 1991. Further inquiry into the cryobehavior of aqueous solutions  
540 of glycerol. Cryobiology 28, 268–278. doi:10.1016/0011-2240(91)90032-J

- 541 Coate, J.E., Luciano, A.K., Seralathan, V., Minchew, K.J., Owens, T.G., Doyle, J.J.,  
542 2012. Anatomical, biochemical, and photosynthetic responses to recent  
543 allopolyploidy in *Glycine dolichocarpa* (Fabaceae). *Am. J. Bot.* 99, 55–67.  
544 doi:10.3732/ajb.1100465
- 545 Coate, J.E., Schlueter, J.A., Whaley, A.M., Doyle, J.J., 2011. Comparative evolution of  
546 photosynthetic genes in response to polyploid and nonpolyploid duplication. *Plant*  
547 *Physiol.* 155, 2081–2095. doi:10.1104/pp.110.169599
- 548 De Castro, M., Martín-Vide, J., Alonso, S., 2005. The climate of Spain: past, present  
549 and scenarios for the 21st century, in: *A Preliminary Assessment of the Impacts in*  
550 *Spain Due to the Effects of Climate Change*. Ministerio de Medio Ambiente,  
551 Madrid, pp. 1–62.
- 552 Demmig-Adams, B., Adams, W.W., 2006. Photoprotection in an ecological context: the  
553 remarkable complexity of thermal energy dissipation. *New Phytol.* 172, 11–21.  
554 doi:10.1111/j.1469-8137.2006.01835.x
- 555 Demmig-Adams, B., Stewart, J.J., Adams, W.W., 2017. Environmental regulation of  
556 intrinsic photosynthetic capacity: an integrated view. *Curr. Opin. Plant Biol.* 37,  
557 34–41. doi:10.1016/j.pbi.2017.03.008
- 558 Duarte, B., Santos, D., Marques, J.C., Caçador, I., 2015. Impact of heat and cold events  
559 on the energetic metabolism of the C<sub>3</sub> halophyte *Halimione portulacoides*. *Estuar.*  
560 *Coast. Shelf Sci.* 167, 166–177. doi:10.1016/j.ecss.2015.10.003
- 561 Ducruet, J.-M., Peeva, V., Havaux, M., 2007. Chlorophyll thermofluorescence and  
562 thermoluminescence as complementary tools for the study of temperature stress in  
563 plants. *Photosynth. Res.* 93, 159–171. doi:10.1007/s11120-007-9132-x
- 564 Ensminger, I., Busch, F., Huner, N.P.A., 2006. Photostasis and cold acclimation:  
565 sensing low temperature through photosynthesis. *Physiol. Plant.* 126, 28–44.  
566 doi:10.1111/j.1399-3054.2005.00627.x
- 567 Ensminger, I., Sveshnikov, D., Campbell, D.A., Funk, C., Jansson, S., Lloyd, J.,



- 568 Shibistova, O., Öquist, G., 2004. Intermittent low temperatures constrain spring  
569 recovery of photosynthesis in boreal Scots pine forests. *Glob. Chang. Biol.* 10,  
570 995–1008. doi:10.1111/j.1365-2486.2004.00781.x
- 571 Fonseca, D., Carvalho, M.J., Marta-Almeida, M., Melo-Gonçalves, P., Rocha, A., 2016.  
572 Recent trends of extreme temperature indices for the Iberian Peninsula. *Phys.*  
573 *Chem. Earth* 94, 66–76. doi:10.1016/j.pce.2015.12.005
- 574 Furió, D., Meneu, V., 2011. Analysis of extreme temperatures for four sites across  
575 Peninsular Spain. *Theor. Appl. Climatol.* 104, 83–99. doi:10.1007/s00704-010-  
576 0324-5
- 577 Gallego, M.J., 1986. Una nueva especie de *Dianthus* del litoral del SW de España.  
578 *Lagascalia* 14, 71–72.
- 579 Garab, G., 2014. Hierarchical organization and structural flexibility of thylakoid  
580 membranes. *Biochim. Biophys. Acta* 1837, 481–494.  
581 doi:10.1016/j.bbabi.2013.12.003
- 582 Giorgi, F., Lionello, P., 2008. Climate change projections for the Mediterranean region.  
583 *Glob. Planet. Change* 63, 90–104. doi:10.1016/j.gloplacha.2007.09.005
- 584 Goltsev, V., Zaharieva, I., Chernev, P., Strasser, R.J., 2009. Delayed fluorescence in  
585 photosynthesis. *Photosynth. Res.* 101, 217–232. doi:10.1007/s11120-009-9451-1
- 586 Guo, W., Yang, J., Sun, X.-D., Chen, G.-J., Yang, Y.-P., Duan, Y.-W., 2016.  
587 Divergence in eco-physiological responses to drought mirrors the distinct  
588 distribution of *Chamerion angustifolium* cytotypes in the Himalaya–Hengduan  
589 mountains region. *Front. Plant Sci.* 7, 1329. doi:10.3389/fpls.2016.01329
- 590 Guo, Y., Tan, J., 2013. Applications of delayed fluorescence from photosystem II.  
591 *Sensors* 13, 17332–17345. doi:10.3390/s131217332
- 592 Hatfield, J.L., Prueger, J.H., 2015. Temperature extremes: effect on plant growth and  
593 development. *Weather Clim. Extrem.* 10, 4–10. doi:10.1016/j.wace.2015.08.001

- 594 Havaux, M., Lannoye, R., 1983. Temperature dependence of delayed chlorophyll  
595 fluorescence in intact leaves of higher plants. A rapid method for detecting the  
596 phase transition of thylakoid membrane lipids. *Photosynth. Res.* 4, 257–263.
- 597 He, Q., Bertness, M.D., Altieri, A.H., 2013. Global shifts towards positive species  
598 interactions with increasing environmental stress. *Ecol. Lett.* 16, 695–706.  
599 doi:10.1111/ele.12080
- 600 Heckathorn, S.A., Ryan, S.L., Baylis, J.A., Wang, D., Hamilton, E.W., Cundiff, L.,  
601 Luthe, D.S., 2002. *In vivo* evidence from an *Agrostis stolonifera* selection  
602 genotype that chloroplast small heat-shock proteins can protect photosystem II  
603 during heat stress. *Funct. Plant Biol.* 29, 933–944.
- 604 Hikosaka, K., Ishikawa, K., Borjigidai, A., Muller, O., Onoda, Y., 2006. Temperature  
605 acclimation of photosynthesis: mechanisms involved in the changes in temperature  
606 dependence of photosynthetic rate. *J. Exp. Bot.* 57, 291–302.  
607 doi:10.1093/jxb/erj049
- 608 Kalaji, H.M., Jajoo, A., Oukarroum, A., Brestic, M., Zivcak, M., Samborska, I.A.,  
609 Cetner, M.D., Łukasik, I., Goltsev, V., Ladle, R.J., 2016. Chlorophyll *a*  
610 fluorescence as a tool to monitor physiological status of plants under abiotic stress  
611 conditions. *Acta Physiol. Plant.* 38, 102. doi:10.1007/s11738-016-2113-y
- 612 Kaplan, F., Kopka, J., Haskell, D.W., Zhao, W., Schiller, K.C., Gatzke, N., Sung, D.Y.,  
613 Guy, C.L., 2004. Exploring the temperature-stress metabolome of *Arabidopsis*.  
614 *Plant Physiol.* 136, 4159–4168. doi:10.1104/pp.104.052142.1
- 615 Klimov, V. V., Baranov, S. V., Allakhverdiev, S.I., 1997. Bicarbonate protects the  
616 donor side of photosystem II against photoinhibition and thermoinactivation. *FEBS*  
617 *Lett.* 418, 243–246. doi:10.1016/S0014-5793(97)01392-6
- 618 Lau, N.C., Nath, M.J., 2014. Model simulation and projection of European heat waves  
619 in present-day and future climates. *J. Clim.* 27, 3713–3730. doi:10.1175/JCLI-D-  
620 13-00284.1

- 621 Levin, D.A., 2002. The role of chromosomal change in plant evolution. Oxford  
622 University Press, New York.
- 623 Li, W.D., Hu, X., Liu, J.K., Jiang, G.M., Li, O., Xing, D., 2011. Chromosome doubling  
624 can increase heat tolerance in *Lonicera japonica* as indicated by chlorophyll  
625 fluorescence imaging. *Biol. Plant.* 55, 279–284. doi:10.1007/s10535-011-0039-1
- 626 Logan, B.A., Demmig-Adams, B., Rosenstiel, T.N., Adams, W.W., 1999. Effect of  
627 nitrogen limitation on foliar antioxidants in relationship to other metabolic  
628 characteristics. *Planta* 209, 213–220. doi:10.1007/s004250050625
- 629 López-Jurado, J., Balao, F., Mateos-Naranjo, E., 2016. Deciphering the  
630 ecophysiological traits involved during water stress acclimation and recovery of  
631 the threatened wild carnation, *Dianthus inoxianus*. *Plant Physiol. Biochem.* 109,  
632 397–405. doi:10.1016/j.plaphy.2016.10.023
- 633 López-Jurado, J., Mateos-Naranjo, E., Balao, F., 2019a. Niche divergence and limits to  
634 expansion in the high polyploid *Dianthus broteri* complex. *New Phytol.* 222,  
635 1076–1087. doi:10.1111/nph.15663
- 636 López-Jurado, J., Mateos-Naranjo, E., García-Castaño, J.L., Balao, F., 2019b.  
637 Conditions for translocation of a key threatened species, *Dianthus inoxianus*  
638 Gallego, in the southwestern Iberian Mediterranean forest. *For. Ecol. Manage.* 446,  
639 1–9. doi:10.1016/j.foreco.2019.05.008
- 640 Maeda, H., Song, W., Sage, T.L., DellaPenna, D., 2006. Tocopherols play a crucial role  
641 in low-temperature adaptation and phloem loading in *Arabidopsis*. *Plant Cell* 18,  
642 2710–2732. doi:10.1105/tpc.105.039404
- 643 Mao, H., Chen, M., Su, Y., Wu, N., Yuan, M., Yuan, S., Brestic, M., Zivcak, M.,  
644 Zhang, H., Chen, Y., 2018. Comparison on photosynthesis and antioxidant defense  
645 systems in wheat with different ploidy levels and octoploid Triticale. *Int. J. Mol.*  
646 *Sci.* 19, 3006. doi:10.3390/ijms19103006
- 647 Marchant, D.B., Soltis, D.E., Soltis, P.S., 2016. Patterns of abiotic niche shifts in

- 648 allopolyploids relative to their progenitors. *New Phytol.* 212, 708–718.  
649 doi:10.1111/nph.14069
- 650 Martínez, L.M., Fernández-Ocaña, A., Rey, P.J., Salido, T., Amil-Ruiz, F., Manzaneda,  
651 A.J., 2018. Variation in functional responses to water stress and differentiation  
652 between natural allopolyploid populations in the *Brachypodium distachyon* species  
653 complex. *Ann. Bot.* 121, 1369–1382. doi:10.1093/aob/mcy037
- 654 Mathur, S., Agrawal, D., Jajoo, A., 2014. Photosynthesis: response to high temperature  
655 stress. *J. Photochem. Photobiol. B Biol.* 137, 116–126.  
656 doi:10.1016/j.jphotobiol.2014.01.010
- 657 Mathur, S., Jajoo, A., Mehta, P., Bharti, S., 2011. Analysis of elevated temperature-  
658 induced inhibition of photosystem II using chlorophyll *a* fluorescence induction  
659 kinetics in wheat leaves (*Triticum aestivum*). *Plant Biol.* 13, 1–6.  
660 doi:10.1111/j.1438-8677.2009.00319.x
- 661 McIntyre, P.J., Strauss, S., 2017. An experimental test of local adaptation among  
662 cytotypes within a polyploid complex. *Evolution.* 71, 1960–1969.  
663 doi:10.1111/evo.13288
- 664 Meng, L.-L., Song, J.-F., Wen, J., Zhang, J., Wei, J.-H., 2016. Effects of drought stress  
665 on fluorescence characteristics of photosystem II in leaves of *Plectranthus*  
666 *scutellarioides*. *Photosynthetica* 54, 414–421. doi:10.1007/s11099-016-0191-0
- 667 Menzel, A., Seifert, H., Estrella, N., 2011. Effects of recent warm and cold spells on  
668 European plant phenology. *Int. J. Biometeorol.* 55, 921–932. doi:10.1007/s00484-  
669 011-0466-x
- 670 Morales, F., Belkhdja, R., Abadía, A., Abadía, J., 2000. Photosystem II efficiency and  
671 mechanisms of energy dissipation in iron-deficient, field-grown pear trees (*Pyrus*  
672 *communis* L.). *Photosynth. Res.* 63, 9–21. doi:10.1023/A:1006389915424
- 673 Murata, N., Takahashi, S., Nishiyama, Y., Allakhverdiev, S.I., 2007. Photoinhibition of  
674 photosystem II under environmental stress. *Biochim. Biophys. Acta* 1767, 414–

- 675 421. doi:10.1016/j.bbabbio.2006.11.019
- 676 Nellaepalli, S., Kodru, S., Subramanyam, R., 2012. Effect of cold temperature on  
677 regulation of state transitions in *Arabidopsis thaliana*. J. Photochem. Photobiol. B  
678 Biol. 112, 23–30. doi:10.1016/j.jphotobiol.2012.04.003
- 679 Ort, D.R., Zhu, X., Melis, A., 2011. Optimizing antenna size to maximize  
680 photosynthetic efficiency. Plant Physiol. 155, 79–85. doi:10.1104/pp.110.165886
- 681 Ottander, C., Campbell, D., Öquist, G., 1995. Seasonal changes in photosystem II  
682 organisation and pigment composition in *Pinus sylvestris*. Planta 197, 176–183.  
683 doi:10.1007/BF00239954
- 684 Oukarroum, A., Goltsev, V., Strasser, R.J., 2013. Temperature effects on pea plants  
685 probed by simultaneous measurements of the kinetics of prompt fluorescence,  
686 delayed fluorescence and modulated 820 nm reflection. PLoS One 8, e59433.  
687 doi:10.1371/journal.pone.0059433
- 688 Oustric, J., Quilichini, Y., Morillon, R., Herbette, S., Luro, F., Giannettini, J., Berti, L.,  
689 Santini, J., 2019. Tetraploid citrus seedlings subjected to long-term nutrient  
690 deficiency are less affected at the ultrastructural, physiological and biochemical  
691 levels than diploid ones. Plant Physiol. Biochem. 135, 372–384.  
692 doi:10.1016/j.plaphy.2018.12.020
- 693 Panchy, N., Lehti-Shiu, M., Shiu, S.-H., 2016. Evolution of gene duplication in plants.  
694 Plant Physiol. 171, 2294–2316. doi:10.1104/pp.16.00523
- 695 Pavlíková, Z., Holá, D., Vlasáková, B., Procházka, T., Münzbergová, Z., 2017.  
696 Physiological and fitness differences between cytotypes vary with stress in a  
697 grassland perennial herb. PLoS One 12, e0188795.  
698 doi:10.1371/journal.pone.0188795
- 699 Penfield, S., 2008. Temperature perception and signal transduction in plants. New  
700 Phytol. 179, 615–628. doi:10.1111/j.1469-8137.2008.02478.x

- 701 Perera-Castro, A. V., Brito, P., González-Rodríguez, A.M., 2018. Changes in thermic  
702 limits and acclimation assessment for an alpine plant by chlorophyll fluorescence  
703 analysis:  $F_v/F_m$  vs.  $R_{fd}$ . *Photosynthetica* 56, 527–536. doi:10.1007/s11099-017-  
704 0691-6
- 705 Pérez-Romero, J.A., Barcia-Piedras, J.-M., Redondo-Gómez, S., Mateos-Naranjo, E.,  
706 2019. Impact of short-term extreme temperature events on physiological  
707 performance of *Salicornia ramosissima* J. Woods under optimal and sub-optimal  
708 saline conditions. *Sci. Rep.* 9, 659. doi:10.1038/s41598-018-37346-4
- 709 Pollastri, S., Jorba, I., Hawkins, T.J., Llusà, J., Michelozzi, M., Navajas, D., Peñuelas,  
710 J., Hussey, P.J., Knight, M.R., Loreto, F., 2019. Leaves of isoprene-emitting  
711 tobacco plants maintain PSII stability at high temperatures. *New Phytol.* 223,  
712 1307–1318. doi:10.1111/nph.15847
- 713 Poudyal, D., Rosenqvist, E., Ottosen, C.-O., 2019. Phenotyping from lab to field -  
714 tomato lines screened for heat stress using  $F_v/F_m$  maintain high fruit yield during  
715 thermal stress in the field. *Funct. Plant Biol.* 46, 44–55. doi:10.1071/FP17317
- 716 R Core Team, 2019. R: a language and environment for statistical computing. R  
717 Foundation for Statistical Computing, Vienna. <https://www.r-project.org/>
- 718 Ramsey, J., 2011. Polyploidy and ecological adaptation in wild yarrow. *PNAS* 108,  
719 7096–7101. doi:10.1073/pnas.1016631108
- 720 Ramsey, J., Ramsey, T.S., 2014. Ecological studies of polyploidy in the 100 years  
721 following its discovery. *Philos. Trans. R. Soc. B Biol. Sci.* 369, 20130352.  
722 doi:10.1098/rstb.2013.0352
- 723 Rochaix, J.-D., 2014. Regulation and dynamics of the light-harvesting system. *Annu.*  
724 *Rev. Plant Biol.* 65, 287–309. doi:10.1146/annurev-arplant-050213-040226
- 725 Salvatori, E., Fusaro, L., Gottardini, E., Pollastrini, M., Goltsev, V., Strasser, R.J.,  
726 Bussotti, F., 2014. Plant stress analysis: application of prompt, delayed chlorophyll  
727 fluorescence and 820 nm modulated reflectance. *Insights from independent*

- 728 experiments. *Plant Physiol. Biochem.* 85, 105–113.  
729 doi:10.1016/j.plaphy.2014.11.002
- 730 Schreiber, U., Schliwa, U., Bilger, W., 1986. Continuous recording of photochemical  
731 and non-photochemical chlorophyll fluorescence quenching with a new type of  
732 modulation fluorometer. *Photosynth. Res.* 10, 51–62. doi:10.1007/BF00024185
- 733 Seehausen, O., 2004. Hybridization and adaptive radiation. *Trends Ecol. Evol.* 19, 198–  
734 207. doi:10.1016/j.tree.2004.01.003
- 735 Sharma, D.K., Andersen, S.B., Ottosen, C.-O., Rosenqvist, E., 2012. Phenotyping of  
736 wheat cultivars for heat tolerance using chlorophyll *a* fluorescence. *Funct. Plant*  
737 *Biol.* 39, 936–947. doi:10.1071/fp12100
- 738 Sharma, D.K., Fernández, J.O., Rosenqvist, E., Ottosen, C.-O., Andersen, S.B., 2014.  
739 Genotypic response of detached leaves versus intact plants for chlorophyll  
740 fluorescence parameters under high temperature stress in wheat. *J. Plant Physiol.*  
741 171, 576–586. doi:10.1016/j.jplph.2013.09.025
- 742 Silva, E.N., Silveira, J.A.G., Ribeiro, R. V., Vieira, S.A., 2015. Photoprotective function  
743 of energy dissipation by thermal processes and photorespiratory mechanisms in  
744 *Jatropha curcas* plants during different intensities of drought and after recovery.  
745 *Environ. Exp. Bot.* 110, 36–45. doi:10.1016/j.envexpbot.2014.09.008
- 746 Soltis, D.E., Visger, C.J., Marchant, D.B., Soltis, P.S., 2016. Polyploidy: pitfalls and  
747 paths to a paradigm. *Am. J. Bot.* 103, 1146–1166. doi:10.3732/ajb.1500501
- 748 Song, Q., Chen, Z.J., 2015. Epigenetic and developmental regulation in plant  
749 polyploids. *Curr. Opin. Plant Biol.* 24, 101–109. doi:10.1016/j.pbi.2015.02.007
- 750 Song, Y.G., Liu, B., Wang, L.F., Li, M.H., Liu, Y., 2006. Damage to the oxygen-  
751 evolving complex by superoxide anion, hydrogen peroxide, and hydroxyl radical in  
752 photoinhibition of photosystem II. *Photosynth. Res.* 90, 67–78.  
753 doi:10.1007/s11120-006-9111-7

- 754 Strasser, R.J., Tsimilli-Michael, M., Srivastava, A., 2004. Analysis of the chlorophyll *a*  
755 fluorescence transient, in: Papageorgiou, G.C., Govindjee (Eds.), Chlorophyll  
756 Fluorescence: A Signature of Photosynthesis. Springer, Dordrecht, pp. 321–362.  
757 doi:[https://doi.org/10.1007/978-1-4020-3218-9\\_12](https://doi.org/10.1007/978-1-4020-3218-9_12)
- 758 Takahashi, S., Murata, N., 2008. How do environmental stresses accelerate  
759 photoinhibition? Trends Plant Sci. 13, 178–182. doi:[10.1016/j.tplants.2008.01.005](https://doi.org/10.1016/j.tplants.2008.01.005)
- 760 Vyas, P., Bisht, M.S., Miyazawa, S.-I., Yano, S., Noguchi, K., Terashima, I.,  
761 Funayama-Noguchi, S., 2007. Effects of polyploidy on photosynthetic properties  
762 and anatomy in leaves of *Phlox drummondii*. Funct. Plant Biol. 34, 673–682.  
763 doi:[10.1071/fp07020](https://doi.org/10.1071/fp07020)
- 764 Wahid, A., Gelani, S., Ashraf, M., Foolad, M.R., 2007. Heat tolerance in plants: an  
765 overview. Environ. Exp. Bot. 61, 199–223. doi:[10.1016/j.envexpbot.2007.05.011](https://doi.org/10.1016/j.envexpbot.2007.05.011)
- 766 Wang, J., Xing, D., Zhang, L., Jia, L., 2007. A new principle photosynthesis capacity  
767 biosensor based on quantitative measurement of delayed fluorescence *in vivo*.  
768 Biosens. Bioelectron. 22, 2861–2868. doi:[10.1016/j.bios.2006.12.007](https://doi.org/10.1016/j.bios.2006.12.007)
- 769 Wei, N., Cronn, R., Liston, A., Ashman, T.-L., 2019. Functional trait divergence and  
770 trait plasticity confer polyploid advantage in heterogeneous environments. New  
771 Phytol. 221, 2286–2297. doi:[10.1111/nph.15508](https://doi.org/10.1111/nph.15508)
- 772 Weiss-Schneeweiss, H., Emadzade, K., Jang, T.-S., Schneeweiss, G.M., 2013.  
773 Evolutionary consequences, constraints and potential of polyploidy in plants.  
774 Cytogenet. Genome Res. 140, 137–150. doi:[10.1159/000351727](https://doi.org/10.1159/000351727)
- 775 Xu, D.-Q., Chen, Y., Chen, G.-Y., 2015. Light-harvesting regulation from leaf to  
776 molecule with the emphasis on rapid changes in antenna size. Photosynth. Res.  
777 124, 137–158. doi:[10.1007/s11120-015-0115-z](https://doi.org/10.1007/s11120-015-0115-z)
- 778 Xu, H., Liu, Guojie, Liu, Guotian, Yan, B., Duan, W., Wang, L., Li, S., 2014.  
779 Comparison of investigation methods of heat injury in grapevine (*Vitis*) and  
780 assessment to heat tolerance in different cultivars and species. BMC Plant Biol. 14,



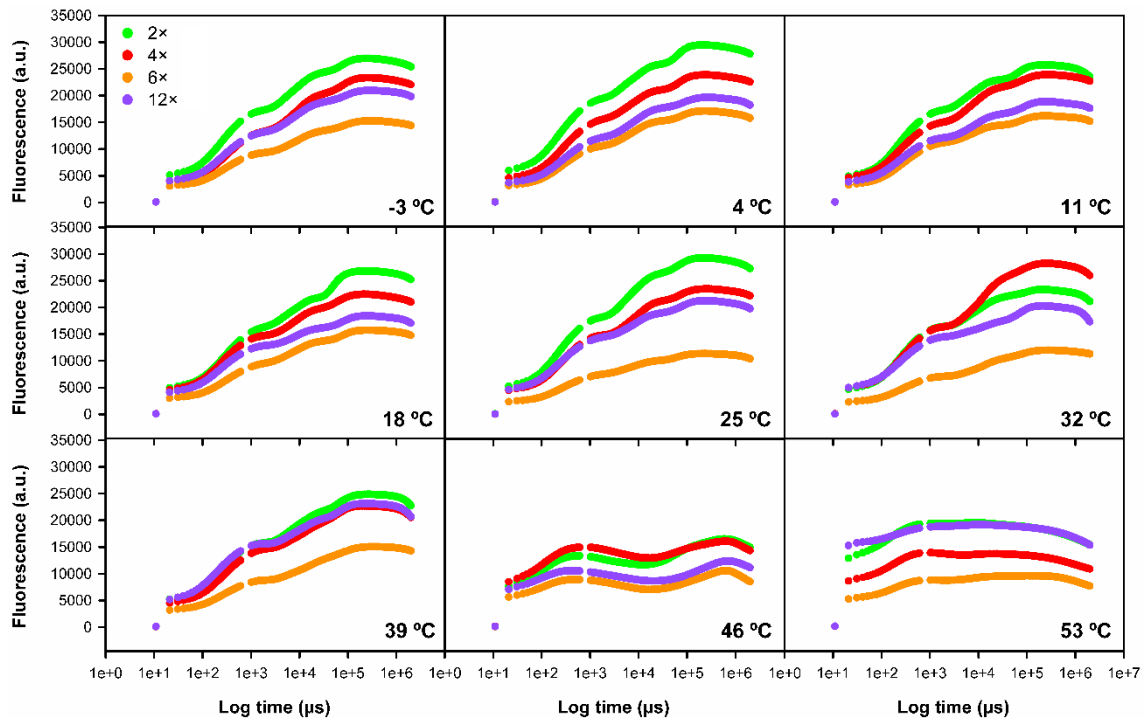
- 781 156. doi:10.1186/1471-2229-14-156
- 782 Yamamoto, Yasusi, Aminaka, R., Yoshioka, M., Khatoon, M., Komayama, K.,  
783 Takenaka, D., Yamashita, A., Nijo, N., Inagawa, K., Morita, N., Sasaki, T.,  
784 Yamamoto, Yoko, 2008. Quality control of photosystem II: impact of light and  
785 heat stresses. *Photosynth. Res.* 98, 589–608. doi:10.1007/s11120-008-9372-4
- 786 Yamane, Y., Kashino, Y., Koike, H., Satoh, K., 1997. Increases in the fluorescence  $F_0$   
787 level and reversible inhibition of Photosystem II reaction center by high-  
788 temperature treatments in higher plants. *Photosynth. Res.* 52, 57–64.  
789 doi:10.1023/A:1005884717655
- 790 Yamane, Y., Shikanai, T., Kashino, Y., Koike, H., Satoh, K., 2000. Reduction of  $Q_A$  in  
791 the dark: another cause of fluorescence  $F_0$  increases by high temperatures in higher  
792 plants. *Photosynth. Res.* 63, 23–34. doi:10.1023/A:1006350706802
- 793 Zhang, L., Xing, D., 2008. Rapid determination of the damage to photosynthesis caused  
794 by salt and osmotic stresses using delayed fluorescence of chloroplasts.  
795 *Photochem. Photobiol. Sci.* 7, 352–360. doi:10.1039/b714209a
- 796

797 **SUPPLEMENTARY MATERIAL**

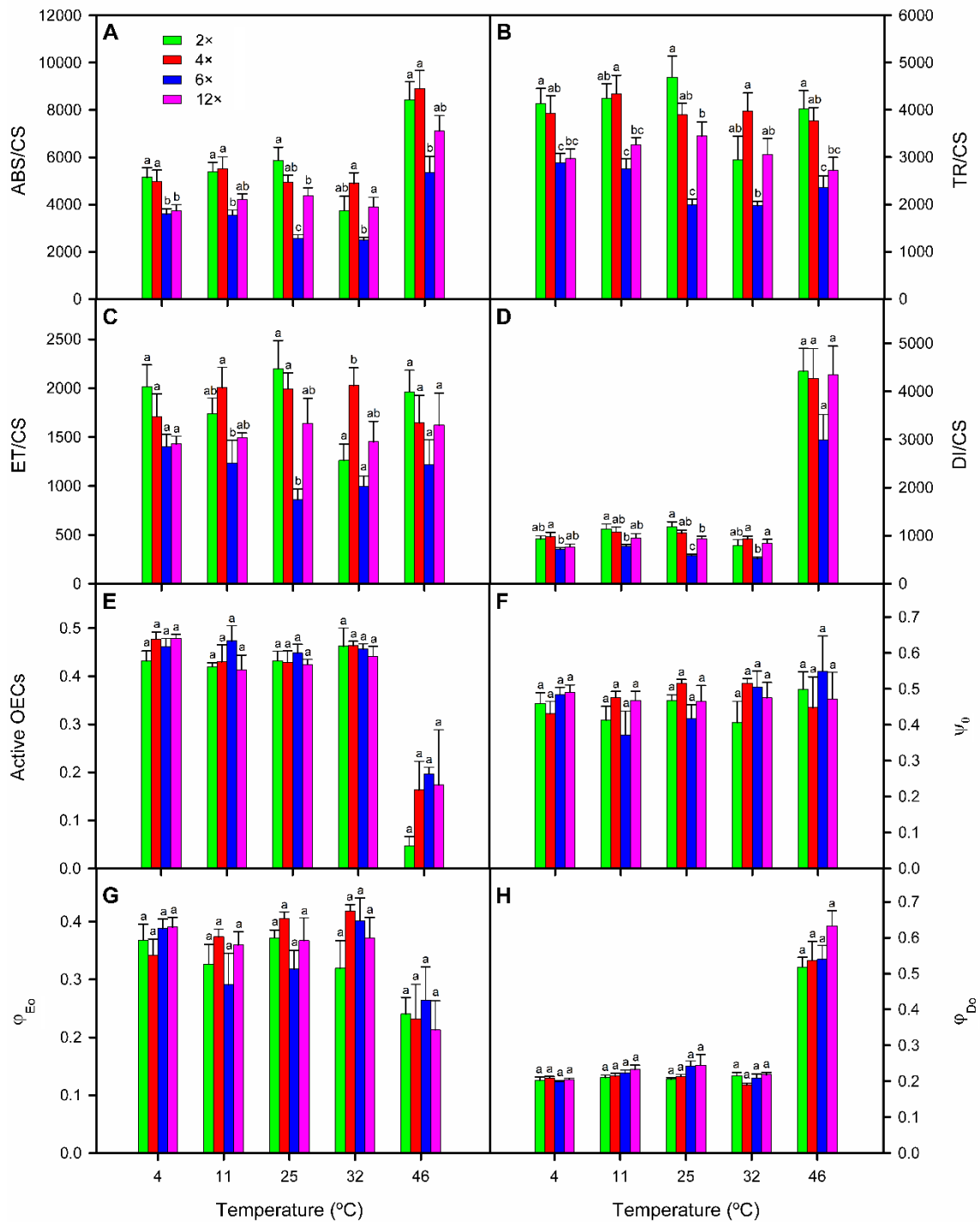
798 **Table S1**

799 Summary of inter-cytotype comparisons in  $F_0$ ,  $F_{\sqrt{F_m}}$  and delayed fluorescence  
 800 (cps/mm<sup>2</sup>) for the different temperature conditions. For each temperature, letters marked  
 801 in bold indicate a significant effect of ploidy level on the response variable (one-way  
 802 ANOVA:  $P < 0.05$ ). Different letters show significant differences among cytotypes  
 803 within each temperature level (Tukey's HSD test:  $\alpha = 0.05$ ).

T (°C)	$F_0$				$F_{\sqrt{F_m}}$				Delayed fluorescence			
	2×	4×	6×	12×	2×	4×	6×	12×	2×	4×	6×	12×
-3	a	a	a	a	a	a	a	a	<b>ab</b>	<b>a</b>	<b>b</b>	<b>ab</b>
4	<b>a</b>	<b>a</b>	<b>b</b>	<b>ab</b>	<b>a</b>	<b>a</b>	<b>a</b>	<b>b</b>	<b>a</b>	<b>a</b>	<b>b</b>	<b>a</b>
11	a	a	a	a	<b>a</b>	<b>b</b>	<b>b</b>	<b>a</b>	<b>a</b>	<b>b</b>	<b>b</b>	<b>a</b>
18	a	a	a	a	a	a	a	a	a	a	a	a
25	<b>ab</b>	<b>ab</b>	<b>a</b>	<b>b</b>	<b>a</b>	<b>a</b>	<b>a</b>	<b>b</b>	a	a	a	a
32	a	a	a	a	a	a	a	a	<b>a</b>	<b>b</b>	<b>a</b>	<b>a</b>
39	<b>a</b>	<b>a</b>	<b>b</b>	<b>a</b>	<b>a</b>	<b>a</b>	<b>b</b>	<b>a</b>	<b>a</b>	<b>b</b>	<b>c</b>	<b>ac</b>
46	<b>a</b>	<b>a</b>	<b>b</b>	<b>a</b>	<b>a</b>	<b>ab</b>	<b>b</b>	<b>b</b>	a	a	a	a
53	<b>a</b>	<b>a</b>	<b>b</b>	<b>a</b>	<b>ab</b>	<b>a</b>	<b>c</b>	<b>b</b>	a	a	a	a



804  
 805 **Fig. S1.** Fluorescence transients (Kautsky curves) in dark-adapted leaves of the four *D.*  
 806 *broteri* cytotypes exposed to nine different temperatures (average values).



807

808 **Fig. S2.** Absorbed energy flux per leaf cross-section, ABS/CS (A), trapped energy flux  
 809 per leaf cross-section, TR/CS (B), transport energy flux per leaf cross-section, ET/CS  
 810 (C), dissipated energy flux per leaf cross-section, DI/CS (D), active oxygen-evolving  
 811 complexes, OECs (E), probability of a PSII trapped electron to be transported from  $Q_A$   
 812 to  $Q_B$ ,  $\psi_0$  (F), probability that an absorbed photon will move an electron into the  
 813 electronic transport chain,  $\phi_{E_0}$  (G), and quantum yield of the non-photochemical  
 814 reactions,  $\phi_{D_0}$  (H), in dark-adapted leaves of the four *D. broteri* cytotypes exposed to

815 five selected temperature levels of the complete range. Parameters were derived from  
816 measurements taken with FluorPen FP100. Values represent mean  $\pm$  standard error.  
817 Different letters indicate cytotypes that are significantly different from each other within  
818 each temperature level (one-way ANOVA:  $P < 0.05$ , Tukey's HSD test:  $\alpha = 0.05$ ).

**Declaration of interests**

The authors declare that they have no known competing financial interests or personal relationships that could have appeared to influence the work reported in this paper.

The authors declare the following financial interests/personal relationships which may be considered as potential competing interests:

### **CRedit authorship contribution statement**

**Javier López-Jurado:** Methodology, Writing – original draft & review and editing, Formal analysis, Investigation. **Francisco Balao:** Conceptualization, Supervision, Validation, Writing – review and editing. **Enrique Mateos-Naranjo:** Conceptualization, Supervision, Validation, Writing – review and editing.